GNSS/INS Sensor Fusion with On-Board Vehicle Sensors

Ryan Dixon, *Hexagon | NovAtel*
Michael Bobye, *Hexagon | NovAtel*
Brett Kruger, *Hexagon | NovAtel*
Jonathan Jacox, *Hexagon | NovAtel*

BIOGRAPHIES

Ryan Dixon is the Sensor Fusion and Autonomy Lead in NovAtel's Applied Research group. In this role he is responsible for exploring sensor fusion methods and relating them to autonomy applications. Prior to this he was Chief Engineer of the SPAN GNSS/INS products group at NovAtel, responsible for the dedicated team maintaining and enhancing NovAtel's inertial product portfolio.

Mike Bobye is a Principal Geomatics engineer at NovAtel Inc. He has a deep breadth of knowledge in GNSS, GNSS/INS integration, and was a member of the original research team that created the first GPS/INS integration at NovAtel in 2000. He has developed several patented methods for improving reliability and robustness of GNSS/INS products.

Brett Kruger is a Software engineer working within NovAtel's Safety Critical group. With his background in INS, Brett leads the development of ASIL rated inertial software targeting autonomous driving applications. Brett graduated with a MASc in Electrical engineering from the University of Toronto in 2012.

Jonathan Jacox is a Senior Research Engineer in NovAtel's Applied Research group. He graduated from the University of Victoria in 2004 with a bachelor's degree in computer engineering, specializing in low-level device drivers and peripheral integration.

ABSTRACT

A key requirement of autonomous vehicle applications is a reliable, accurate, and robust positioning (aka localization) solution. Key navigation, planning and decision operations cannot happen without dependable positioning. This means that accurate positioning must be ubiquitous - in other words, reliably available at all times and in all places the vehicle is expected to operate. While Global Navigation Satellite Systems (GNSS) commonly provide the basis for absolute positioning, it always suffers from the inherent problem of availability whenever a direct view of enough satellites is not possible.

To address the failure mode, additional complementary sensors can be added to the overall navigation solution through a technique known as sensor fusion. Sensors such as inertial measurement units (IMUs), cameras, LiDARs, RADAR, etc. can be selected in such a way that the individual shortcomings of each sensor are mitigated, and the overall robustness and reliability are improved. Although current autonomous vehicle applications employ sensor fusion techniques, they tend to rely on high-performance sensors to meet the accuracy requirements. These high-performance sensors tend to induce a much higher cost burden than would be acceptable for commercial production, and therefore make mass autonomy too expensive.

This paper will focus on the exploitation of the lower cost sensors already available on most modern vehicles. These sensors include low resolution odometry (DMI) and consumer grade IMUs currently used for dynamic stability control and wheel slip detection. A novel approach for combining vehicle speed, steering angles, transmission settings and multiple odometry inputs will be presented along with achievable results while operating under a GNSS denied environment. The test trajectory will mimic a typical parking structure with many corners and short straight segments. The only *apriori* information required for the filter is the wheel track and wheelbase (separation of wheels).

A 90% performance improvement compared to the stand-alone GNSS/INS solution was observed during GNSS outages up to 30 minutes. Furthermore, up to a 50% improvement was observed when comparing between the multi-odometry vs single odometry outages during the same 30-minute outage condition. Beyond GNSS outage performance, it will be shown how the use of the extra input to the filter can improve protection levels of the positioning system to allow for more frequent engagement of the autonomous navigation system.

INTRODUCTION

Any autonomous machine must be safe to operate, meaning it cannot cause any harm to any people and property. The stringency of this requirement does vary somewhat by environment; a packed public street is more difficult to operate safely in than a closed mine site. Whatever the operational environment, extremely reliable solutions are required.

The positioning/localization system is one of many possible components of the overall autonomous system, each of which is expected to meet strict safety requirements. Conversely, to ensure the adoption of such a system in the consumer market it must also cost less than a manual system capable of the performing the same task. Although the overall cost will include ancillary costs such as maintenance and accident rates, the initial investment must not be prohibitive as is true across most commercial industries.

Recent autonomous development has focused primarily on proving out the technology. This process has been underway for the past several years with all the successes, and failures, being well documented in the media. The technology is maturing rapidly with a growing adoption rate, however during the initial phase most of the vehicles have been equipped with high-performance sensors that are simply too expensive for commercial products. The conflict between cost versus accuracy and reliability is driving innovation across the industry to maintain the solution expectations while driving hardware costs down. This paper will primarily focus on the positioning/localization aspect of the problem, by showing how to provide a reliable and robust solution while minimizing the cost of the input sensors.

An obvious way to tackle the cost of the system is to fully utilize existing vehicle sensors. On most modern automobiles produced within the last decade, there are numerous sensors available that have been added for alternate advanced features. Sensors used for stability control, adaptive all-wheel drive, anti-lock brakes, etc. have become available on a wide variety of vehicles during this period. Although the sensors were not intended for positioning purposes, the information they provide can be very useful for such applications. To evaluate the effectiveness of these additional sensors, performance analysis will be provided while operating in a GNSS denied environment using combinations of consumer grade GNSS/INS systems and additional vehicle inputs provided via the vehicle CAN bus.

SENSOR FUSION IN POSITIONING

There are numerous methods for designing a system that can handle a multitude of sensors, each providing their own list of benefits. Due to the inherent, self-contained, aspect of inertial measurement units (IMUs), the filter design used for this discussion focused on the IMU as the nucleus of the sensor fusion positioning system. Although IMUs are independent of the environment within which they operate, they are susceptible to exponential error growth due to the nature of the observations. The errors can be controlled in several ways. The first method involves using higher performance IMUs with much lower error source, however this solution would greatly increase the overall cost of the system. A second method for controlling the errors is by applying complementary update sources, such as GNSS and/or vehicle data information. Once the errors are controlled, a continuous accurate solution for all possible environments will be available from the positioning system.

The dramatic improvement of consumer grade micro-electromechanical sensors (MEMS) over the last several years has greatly improved the ratio of cost to accuracy for IMUs. In addition, multi-frequency low-cost commercial GNSS receivers are also more readily available to be paired with MEMS IMUs. These commercial GNSS receivers are typically designed to track weaker satellite signals, allowing them to track more observations in historically poor GNSS environments. The pairing of consumer GNSS with MEMS inertial sensors can provide an accurate solution in most conditions for a relatively low-cost point. However, MEMs IMU sensors still have limitations with regards to the overall performance they can achieve during update outages. To overcome this limitation, additional information is required. The information can come from historically expensive visual sensors, such as cameras and LiDAR, which also require significant computing power to be used effectively. Or, as discussed earlier, vehicle data information can be utilized to significantly constrain error growth and provide robust outlier detection.

Modern vehicles already possess a wealth of additional sensor information from other subsystems such as Antilock Braking Systems (ABS) and Dynamic Stability Control (DSC). These sensors can be harnessed to improve the GNSS/INS solution at no additional cost and minimal computing power. With access to the high-speed data bus of a vehicle, multiple odometers, steering wheel angles, transmission settings, vehicle speed sensors and more can be accessed. These redundant measurements can be used to significantly constrain inertial error growth and in outlier detection. This is particularly helpful in traditionally difficult GNSS conditions such as parking structures, tunnels, urban canyons, orchards, etc.

FUNCTIONALLY SAFE OPERATION

In addition to providing additional accuracy, fusing the vehicle sensor data into the INS positioning algorithm also allows for a reduction in protection levels (PLs). PLs are a metric used in safety critical applications designed to represent the maximum possible error that may be present in the system, up to a high degree of confidence [1]. A PL has a corresponding integrity risk, which represents the maximum allowable failure rate, and is typically represented in failures per hour. A typical integrity risk of 10^{-7} per hour is used in this paper, meaning the error will only exceed the protection level once in 10^{7} hours of operation. Protection levels are typically compared to an alert limit (AL) to decide whether the position solution is currently safe to use in autonomous applications. An AL would be set by an integrator and represents the largest error that can be present in the positioning output for it to still be a useful input for autonomous decision making. In autonomous driving, for instance, alert limits of 2-5 metres are common, representing lane-level, or road-level positioning confidence.

Using tactical grade IMUs allows near seamless PL bridging through short GNSS outages [2]. However, using low-cost hardware to meet the needs of mass-market deployment, PLs tend to grow very fast during GNSS outages. This is because the PL needs to represent the worst-case error growth during periods of inertial navigation, due to estimation errors at the start of the outage plus random noise and sensor error drifts during the outage. In addition to constraining error, adding vehicle information provides a redundant input into the positioning algorithm, which helps to reduce the PL growth.

The final test of the paper will use automotive grade GNSS and INS sensors to illustrate the PL behaviour in a typical automotive environment, and how this behaviour is affected by the addition of vehicle sensor information.

VEHICLE DATA INTEGRATION

Mandatory Dynamic Stability Control (DSC) aka Electronic Stability Control (ESC) came into effect in the United States in 2012 [3] and Europe in 2014 [4]. Vehicles produced after this time all include a similar set of sensors to enable this functionality. These sensors are used for stability and slip detection as well as other monitoring and control functions (emergency braking, for example). They include relatively high-fidelity odometers on each wheel, multiple vehicle speed sensors, steering wheel angle sensors, transmission settings and potentially more.

Although the primary purpose of these sensors is to provide stability control functionality, many of them can provide valuable information for positioning. A major difficulty to overcome is accessing the data from the individual sensors externally. They were not designed for external use and the data typically resides on the closed internal high-speed data bus of the vehicle. One method of access to the information lies with the on-board diagnostic (OBD) interface. The underlying problem with the OBD is it was designed for diagnostics and the data access is at a much lower output rate and priority. The ideal solution is to establish a direct connection to the vehicle’s high-speed internal data bus.

All testing was done using a Lexus RX450h outfitted with a Hexagon | AutonomousStuff PACMod (Platform Actuation and Control Module) drive-by-wire system. The PACMod system provides a method for easy access to the vehicle’s internal high-speed data bus over a CAN interface, or through a ROS driver. Figure 1 shows the vehicle used for all data collection and testing.

Figure 1 – Hexagon | AutonomouStuff Equipped Lexus RX450h Test Vehicle

Vehicle data sensors and internal high-speed data bus provide an attractive solution to adding more information to the positioning filter while maintaining a solution that is as cost-effective as possible. It must be understood that the available sensors were selected to complete their DSC related tasks and are therefore not intended specifically for navigation purposes. Vehicle dynamics and ground conditions (i.e. wheel slip) can directly affect the stability of the observations. Therefore, fusing the individual sources into reliable INS updates requires significant work to ensure erroneous measurements do not corrupt the final solution. Often these techniques can result in limitations with regards to the amount of weight, or trust, each sensor is given during updates. So, although these sensors provide extremely useful information, they cannot provide centimeter level positioning on their own. Rather they provide a mitigation in INS error growth and some form of redundancy to the overall solution for improved protection levels and greater solution consistency.

An informative break down of the primary aiding sensors available from the vehicle data will be provided in the following sub-sections.

Differential Odometry

A sensor used for measuring distance is generally referred to as a distance measurement instrument or DMI. Odometry is a form of DMI and on most vehicles is done by mounting odometers on one or more wheels of the vehicle to measure the amount of wheel rotation. The measured distance from the DMI is used by the inertial filter as either a position or velocity update.

The advantage of having simultaneous odometry for all the wheels is it allows for a process known as differential odometry. From the multiple sensor readings, redundancy and measurement quality can be greatly improved. Furthermore, new information is inherently provided, such as relative yaw rate measurements by differencing wheel rotation rates [5]. Although differential odometry is not a new concept, using it effectively is challenging. It requires *apriori* knowledge of the platform on which it is operating. For example, the test vehicle used in this case was a road vehicle employing front wheel Ackermann steering [6], illustrated in Figure 2. However, vehicles using other steering methods, such as skid-steer or articulated, will exhibit different wheel behaviour resulting in alternative modelling requirements.

Historically, odometry measurements were limited to a single wheel, providing one distance measurement per sample, but with the DSC systems on modern cars, there are odometers on all wheels. This allows for the simultaneous use of data from all the wheels, a process called differential odometry. This allows for better distance measurements via redundancy and additionally provides relative yaw measurements by differencing wheel rotation rates [5].

Figure 2 represents a typical Ackermann steered vehicle with an arbitrarily IMU placement. This is to illustrate all the necessary offsets and dimensions to be considered during initial setup of the system. Each wheel will experience a different velocity during a turn. To further complicate conditions, the IMU centre of navigation will be experiencing a different velocity to that of all the wheel velocities. Additionally, the angles of the two front wheels will be different during a turn. These differences must be accounted for to use multiple odometers properly.

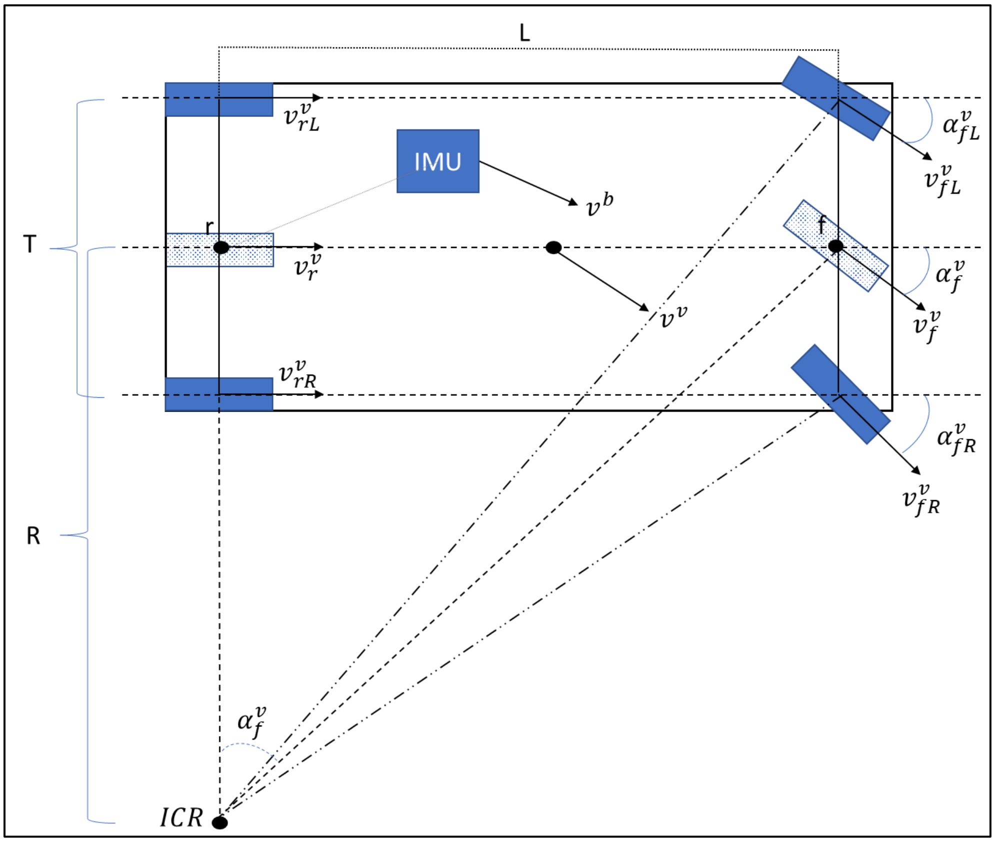

Figure 2 - Wheel Odometers and IMU, Ackermann Steering Vehicle

Where:

T	Vehicle wheel track (width of vehicle defined by centre of left/right tires)
L	Vehicle wheelbase (length of the vehicle defined by centre of front/rear tires)
R	Radius of Turn
ICR	Instantaneous Centre of Rotation
$v_{rR}^v, v_{rL}^v, v_{fR}^v, v_{fL}^v$	Vehicle frame velocity of each wheel; rear right, rear left, front right and front left, respectively
v_r^v, v_f^v	Vehicle frame velocity of virtual centre wheels; rear and front, respectively
v^b	IMU body frame velocity
v^v	Vehicle frame velocity of the vehicle centre
α_f^v	Effective steering angle of the vehicle, defined by virtual front centre tire, relates to the instantaneous centre of rotation
$\alpha_{fR}^v, \alpha_{fL}^v$	Actual steering angle (Ackermann) of right and left front wheels, respectively. The wheel on the inside of the turn will have a larger angle than the outside wheel.

Additional error states must be added to the position filter when dealing with DMI update sources. For example, each wheel could have slightly different measurement scales due to sensor biases and environmental conditions. These differences could cause an apparent scale factor on each of the DMI measurements as the circumference changes.

In order to minimize the number of additional states in the filter and to reduce the angular complexity of the Ackermann steering angles on the front wheels, the distance measurements are made with respect to a virtual centre wheel and all rotations are computed about those points. This is known as the bicycle model. This allows for a reduced number of additional filter states while preserving two unique sets of measurements into the system. Using all four wheels independently provides more unique measurements but requires more estimation states and complexity in order to handle the additional translations. The most effective method may vary depending on the vehicle and environmental conditions, but in road testing, the virtual centre wheel method produced excellent results.

Transmission

Vehicle transmission settings are useful to resolve the ambiguity in initial vehicle direction. This is particularly important for initialization of the INS system, depending on the overall system configuration.

INS systems require an initial position and attitude to begin navigating. The initial azimuth can come from a variety of sources. Tactical grade IMUs can measure Earth's rotation to compute an initial azimuth in a process called static gyro-compassing. However, the grade of sensors used for commercially viable autonomous vehicles cannot effectively measure earth's rotation. This leaves three options for providing the initial azimuth to the INS system. First is that the initial azimuth is provided externally, possibly from memory or from another system. Second is from a dual-antenna GNSS system where the azimuth between the two antennas is computed by GNSS and relayed to the INS. And third is a kinematic alignment where the vehicle's course over ground is used as the initial azimuth source.

All three methods are likely to be used to varying degrees depending on the vehicle size, cost, dynamics etc. However, the only truly independent method is a kinematic alignment method. In this method the initial vehicle direction (forward or reverse) is an unknown. Without any knowledge of the vehicle, this is an ambiguity to an initializing INS system as the IMU cannot know which way is forward on the vehicle.

The SPAN system will attempt to determine the direction by monitoring the raw accelerometer output to determine if the vehicle is accelerating forwards or backwards [7]. This method is reliable but adds time to system initialization as the azimuth direction is verified.

Adding in vehicle transmission information immediately removes this ambiguity. This allows for faster INS system initialization, which in turn reduces the time from ignition to autonomy system engagement.

Vehicle Speed

Vehicle speed measurements may be provided by sensors in addition to the odometers. These can come from a variety of internal places such as driveshaft or differential, or it can come from external sensors such as ground RADAR in some cases. In either case, these provide primarily redundancy to the odometer speeds to help detect wheel slippage or any other erroneous measurements.

Steering Angle / Curvature

The steering angle of a vehicle coupled with a speed measurement can provide a relative yaw measurement. This is also provided by using differential odometry, but like vehicle velocity, these additional sensors provide a redundant measurement for error checking.

The sensors providing steering angle and the method of reporting the angles can vary greatly. Most common is the steering wheel angle, though in some cases the actual wheel angles can be provided. In skid steer or articulated vehicles this becomes more complicated to translate into the turning rate. It is so variable in fact that some standardization bodies have attempted to define specific methods for communicating vehicle turn. For example, the ISO11783 (aka ISOBUS) standard defines their steering message PGN9216 where steering is represented via inverse radius of turn [8].

Depending on the sensors used, the conditions, and the measurement method, the steering angle measurements can be noisy and difficult to use as a navigation aiding source. It is particularly useful for vehicles which move very little as this is the case where INS azimuth accuracy struggles.

TEST EQUIPMENT

The test section of this document covers three test scenarios. The test vehicle used for all tests was discussed above and shown in Figure 1. The customized Lexus RX450h allowed access to the high-speed internal data bus of the Lexus for testing. Regarding the dedicated positioning sensors (GNSS and IMU), two different configurations were used.

For the first two test cases, a Hexagon | NovAtel PwrPak7D-E1 receiver was used. This houses a survey grade dual-antenna GNSS receiver as well as a commercial grade Epson G320N IMU and is a system commonly used in autonomous test vehicles. The final used automotive grade GNSS and IMU sensors. As the focus of the test is on GNSS denied areas, the IMU type is the primary contributor to error growth [9]. In all cases a truth system running another NovAtel PwrPak7D connected to a tactical grade Litef µIMU-IC IMU was used. The truth and PwrPak7-E1 were run in RTK mode while the automotive sensor set used TerraStar X PPP [10]. The equipment used can be seen mounted in the vehicle in Figure 3 below.

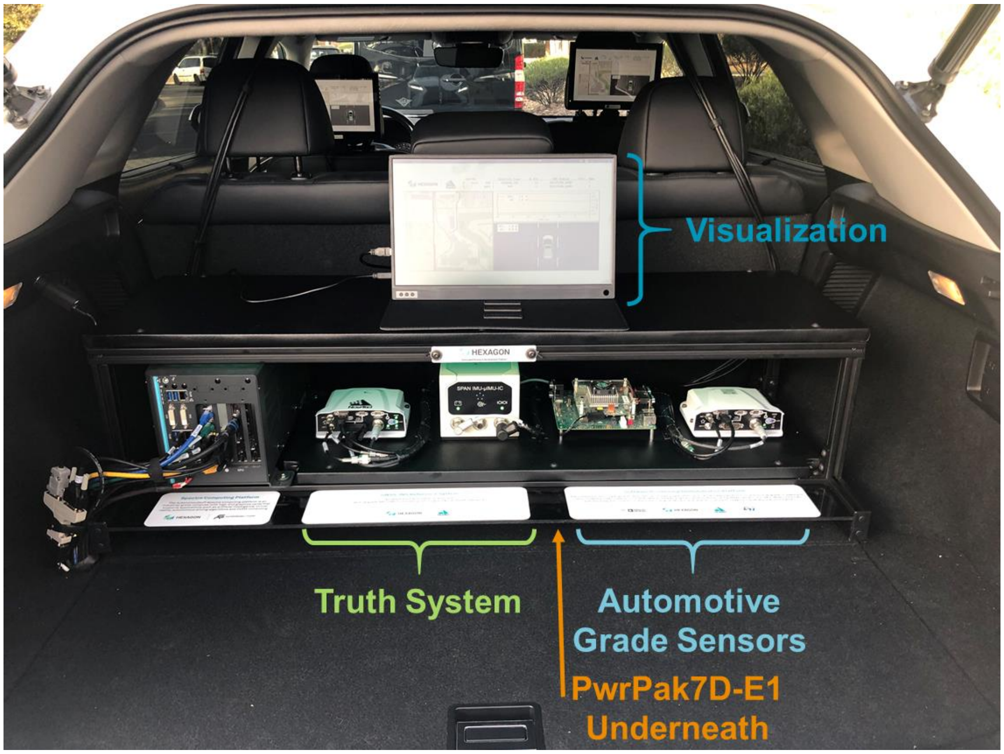

Figure 3 – Test GNSS/INS Equipment in the Test Vehicle

TEST RESULTS

As discussed in the previous section, three test cases are presented, investigating the effects of pairing the INS solution with vehicle sensor data. The first two tests induce large 30-minute GNSS outages on a commercial GNSS/INS receiver under different trajectory types (mixed road and parking structure) to observe error growth. The third also takes place in mixed road conditions but imposes shorter outages on automotive grade sensors to illustrate the effect on both errors and protection levels.

Test 1: Extended GNSS Outages, Road Conditions

The first test scenario takes place in an open sky mixed driving environment. A loop containing highway and suburban driving, including some traffic lights (meaning some zero velocity updates), is driven repeatedly. The test unit is a Hexagon | NovAtel PwrPak7D-E1. It is subjected to a 30-minute GNSS outage, meaning the position is based entirely on IMU and vehicle sensors with full GNSS denial. The control unit provides the reference trajectory and correspondingly does not have GNSS removed, remaining in RTK. In this test, the GNSS outage was induced in post-mission processing to observe the effects with various levels of aiding provided to the INS solution. Results are presented at the 10 and 30-minute marks of GNSS outage.

This test simulates a scenario where GNSS is entirely denied for an extended period in a city. Though outages are unlikely to persist for that long, it could happen due to damage to the GNSS antenna, GNSS jamming, or possibly just extreme sky occlusion from the lower deck of a bridge. The distances and speeds driven are quite large, with an approximate distance travelled of 37 Km through the outage.

To appreciate the scale of errors shown below, it is helpful to understand the baseline performance of an INS filter not applying any constraints through an update outage. Land vehicle constraints [7] are otherwise applied in all remaining results presented herein.

Figure 4 shows the errors which can accumulate over a 10-minute GNSS outage with such an unconstrained INS system using this IMU. The expected second order error growth of the position is easily observed as well as the huge improvements provided by applying land vehicle constraints.

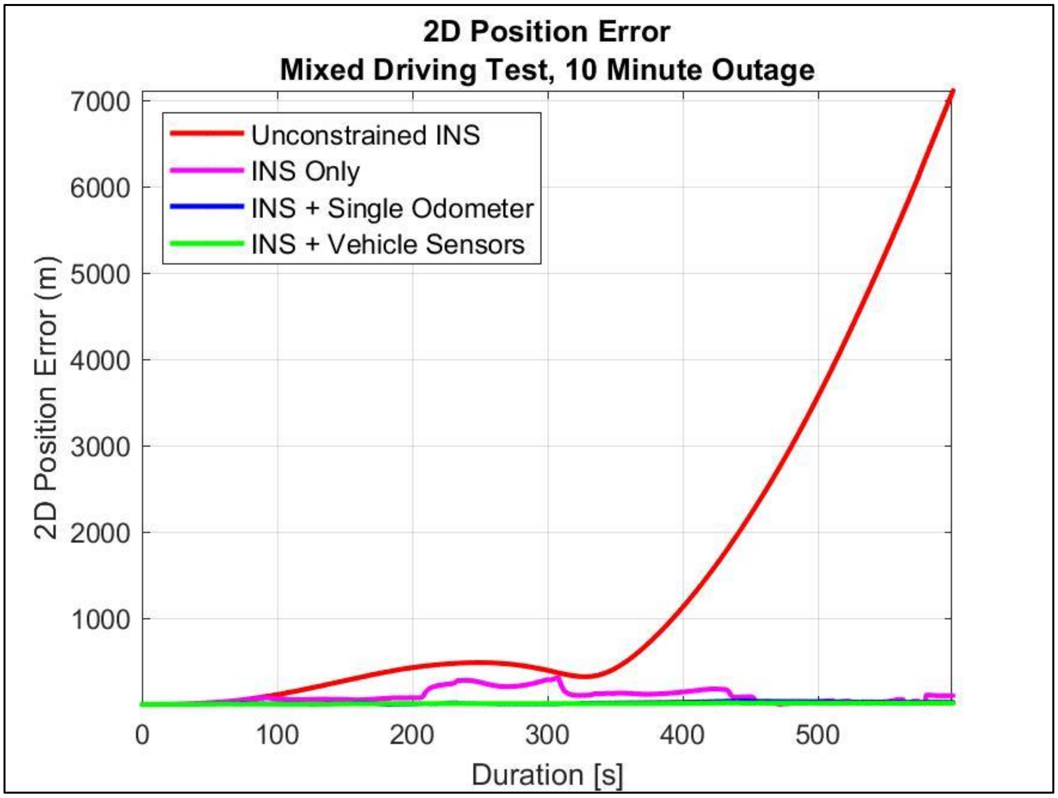

Figure 4 – 2D Position Error of Various INS Configurations

Obviously, it is difficult to visually compare improvements at this scale, so the unconstrained error growth will not be shown for the remainder of the test scenarios. It was included here for context. What will be shown is the INS using land vehicle constraints without aiding sensors, adding a single odometer and full vehicle sensor data. Figure 5 below shows the same data to Figure 4 with the unconstrained data removed.

From this, it is clearly observable that the land vehicle constraints themselves provide an immense benefit over unconstrained INS error growth but are still subject to significant random error accumulation. From there, adding a single odometer and then all the vehicle sensor data continues to improve and stabilize the error growth.

Using a single odometer provides a single distance measurement allows observation of accelerometer errors in the along-track IMU axis (depending on IMU orientation), but not the remaining accelerometers or gyroscopes, so a reduction in error accumulation is observed, but the error growth begins to destabilize as azimuth error accumulates and skews the application of the updates to the across-track accelerometer.

Using differential odometry and redundant sensors allows for both additional distance measurements and relative yaw observations. Doing this allows for more effective distance measurements and observations of the yaw gyro error. This leads to lower error growth and much greater stability throughout the outage. Figure 6 shows the azimuth error of the system during the outage and illustrates how the single odometer has virtually no impact on azimuth error while the full vehicle sensor data significantly constrains it.

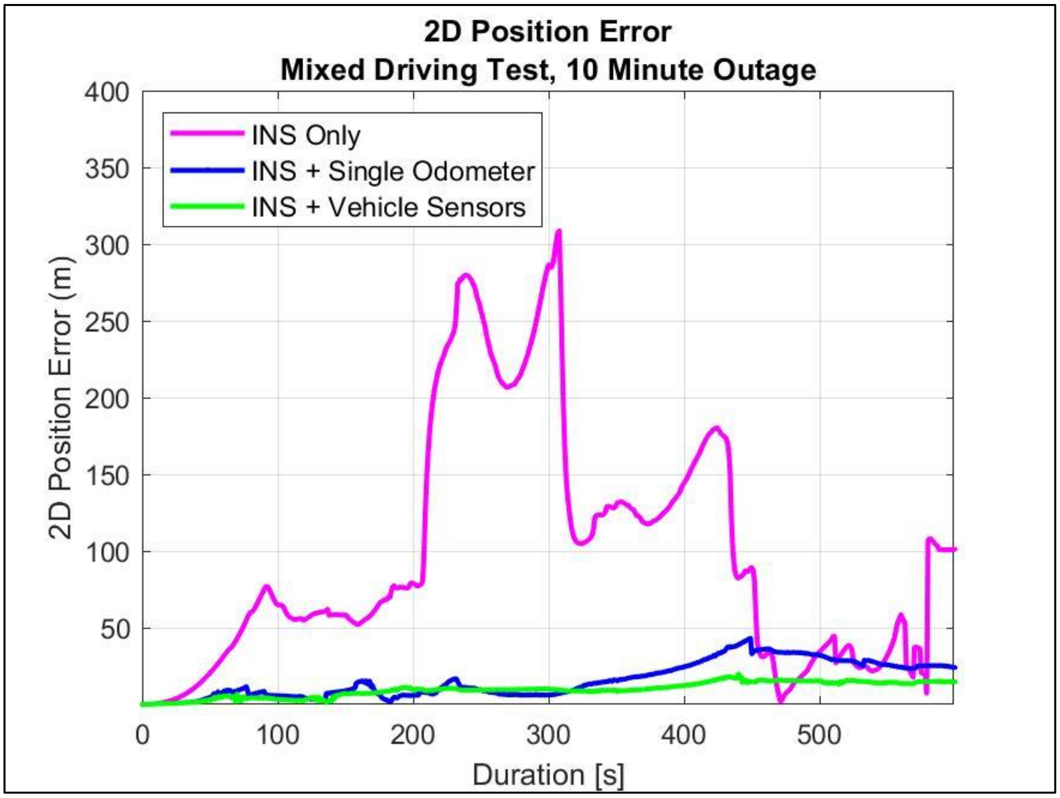

Figure 5 – 2D Position Error Over a 10 Minute GNSS Outage

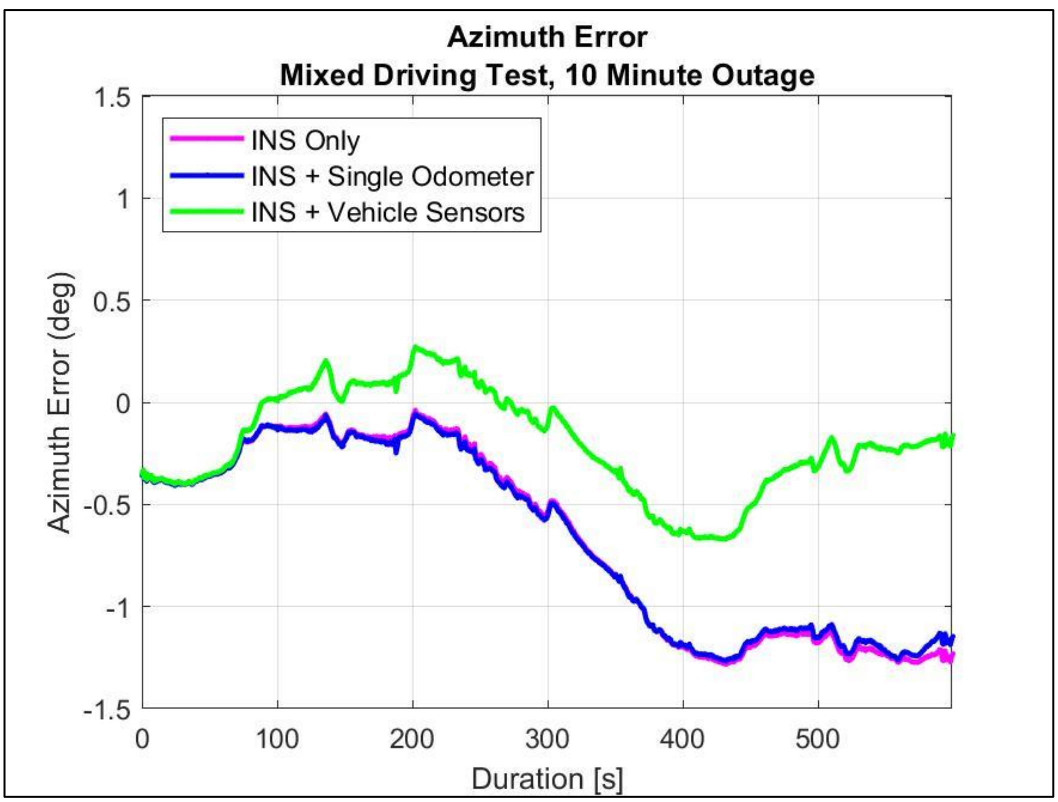

Figure 6 – Azimuth Error Over a 10 Minute GNSS Outage

The numerical RMS and 95% errors of this 10-minute outage are shown in Table 1. The improvements apparent in the preceding plots are also clearly represented in the statistics, particularly for the 95% confidence numbers.

Table 1 10 Minute Outage Error Statistics, Mixed Driving Test

Solution	RMS Error			95% Error		
	2D Position (m)	Height (m)	Azimuth (deg)	2D Position (m)	Height (m)	Azimuth (deg)
Unconstrained INS	2416.57	170.64	0.49	5752.08	385.14	1.50
Land Profile – No DMI	125.36	21.59	0.46	237.08	38.01	1.39
Single Odometer	19.57	2.86	0.44	34.09	5.22	1.33
Vehicle Sensors	10.79	2.31	0.25	14.22	4.47	0.76

Figure 7, Figure 8 and Table 2 show the same data over the full 30-minute outage. These show that the trends observed in the 10-minute outage continue and become even more apparent. The accumulating IMU errors are increasingly reduced as more vehicle sensor data is allowed to help. The azimuth error remains very well bounded throughout this excessive outage.

Another interesting phenomenon can be observed in Table 2, showing that in all positioning modes the vertical error growth is much lower than horizontal. This is typically true of INS systems because the gravity measurement already provides some observables on the vertical accelerometer. Conversely, the addition of vehicle sensors has less impact on this error which also makes sense because they provide no additional measurement on this accelerometer. They do however provide additional attitude constraints, which indirectly reduces the vertical error growth to a smaller degree. Consequently, the plots presented within the paper focus on horizontal (aka 2D) position errors.

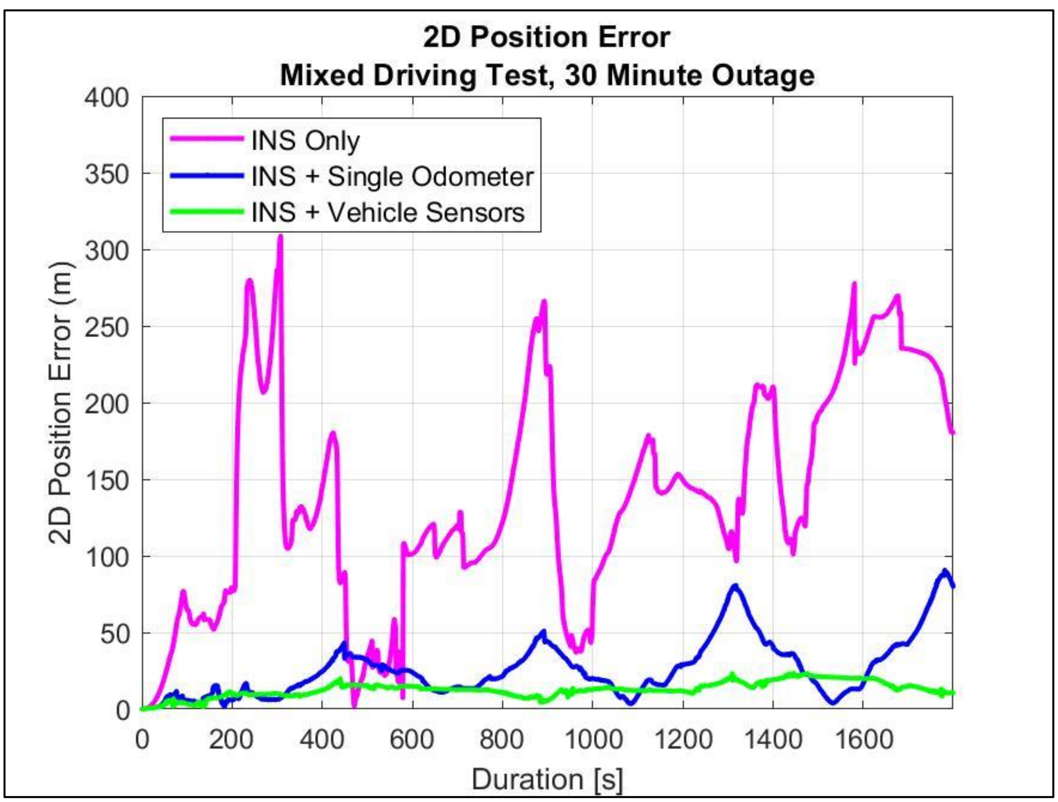

Figure 7 – 2D Position Error Over a 30 Minute GNSS Outage, Mixed Driving Test

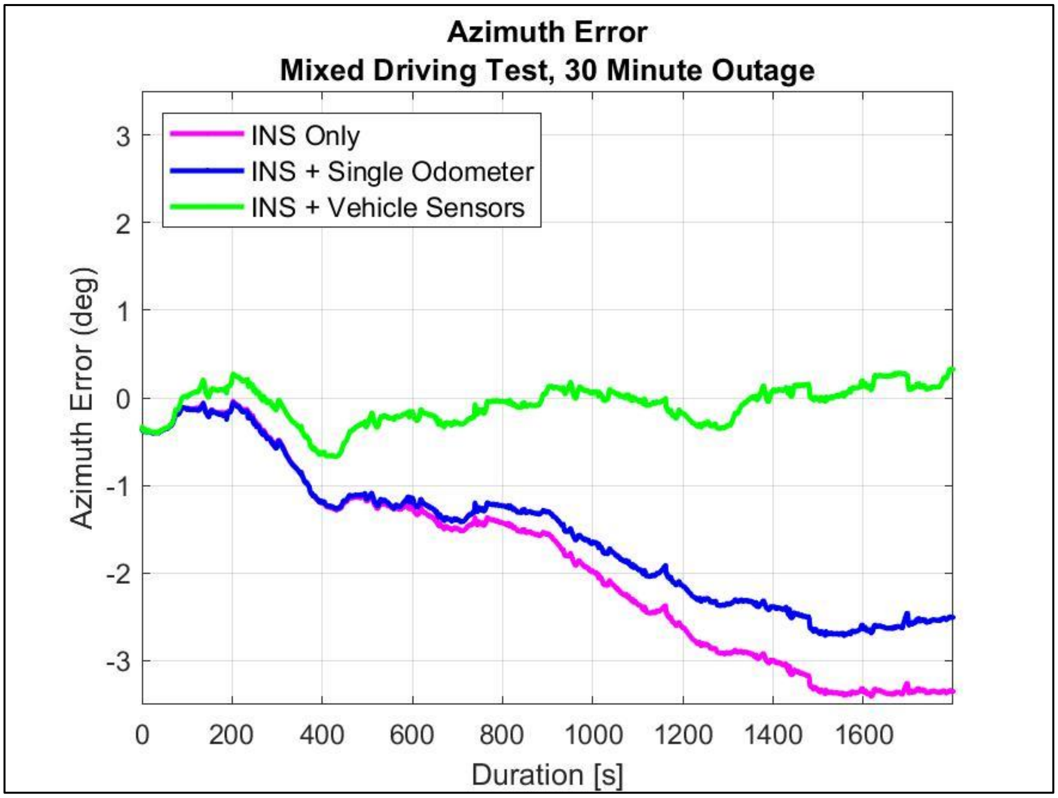

Figure 8 – Azimuth Error Over a 30 Minute GNSS Outage, Mixed Driving Test

Table 2 30 Minute Outage Error Statistics, Mixed Driving Test

Solution	RMS Error			95% Error		
	2D Position (m)	Height (m)	Azimuth (deg)	2D Position (m)	Height (m)	Azimuth (deg)
Land Profile – No DMI	156.33	23.76	1.09	218.01	24.69	3.26
Single Odometer	32.54	4.40	0.81	57.52	12.21	2.43
Vehicle Sensors	13.72	6.23	0.22	14.61	16.03	0.65

Another popular way to represent performance of an INS system is as a measure of error over the distance travelled. This is typically represented as a percentage, where the lower the number, the better. This can be a somewhat misleading statistic for INS systems as error typically grows over time rather than distance, meaning the statistic is heavily influenced by the speed driven for the test. However, it is useful here since the same data was used over the same distance outage so comparisons of overall error growth on the different positioning methods can be compared. These statistics are shown in Table 3, and again the use of vehicle sensor information is a large improvement at all measurement times.

Table 3 Maximum Error / Distance Travelled, Mixed Driving Test

Solution	Maximum 3D Error / Distance Travelled (%) Over Outage Duration (min)			
	1 Min	5 Min	10 Min	30 Min
Unconstrained INS	3.32	6.43	7.12	5.95
Land Profile – No DMI	3.23	5.00	2.71	0.56
Single Odometer	1.00	0.40	0.35	0.29
Vehicle Sensors	0.72	0.42	0.15	0.05

Finally, to look at these results in a map view, this can be seen in Figure 9 below. This provides a clearer idea of what these errors translate to in real world environments. Figure 10 zooms in on the southwest corner which is an off-ramp turn. The control on this section was always in the same lane but even after a full 30-minute outage the INS + vehicle sensor data is still on the roadway.

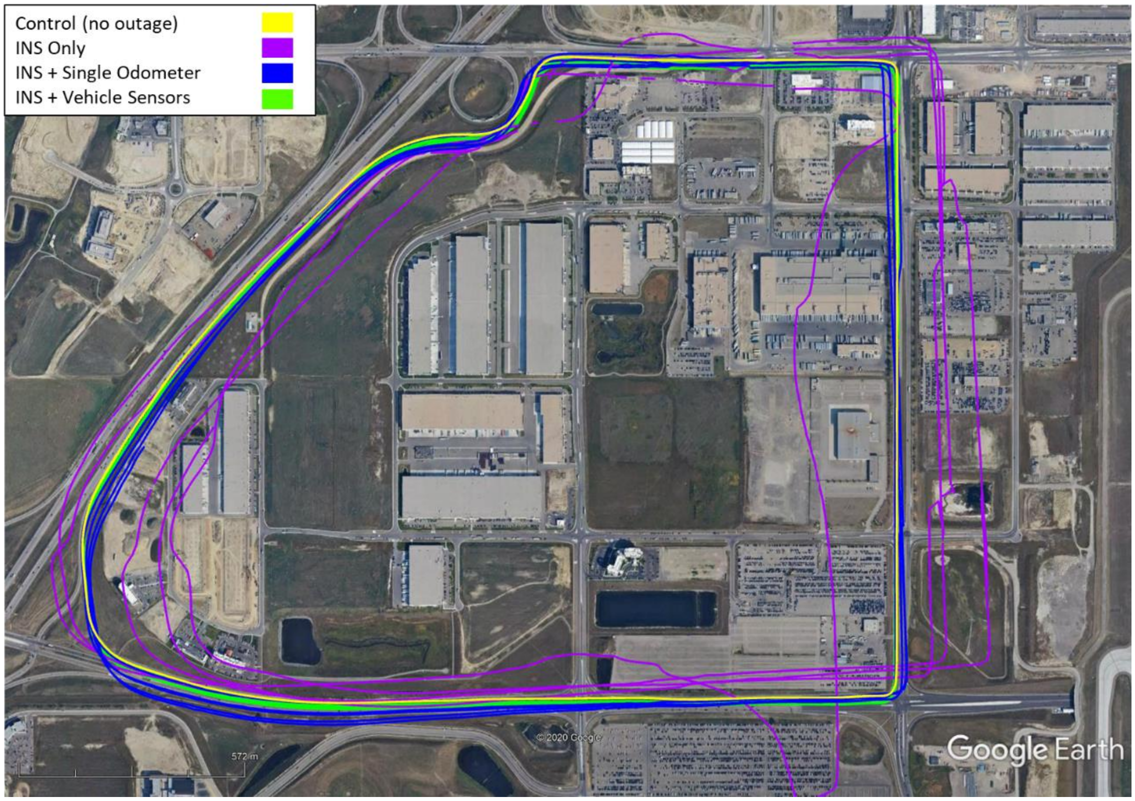

Figure 9 – Map View of 30-Minute GNSS Outage Performance, Mixed Driving Test [11]

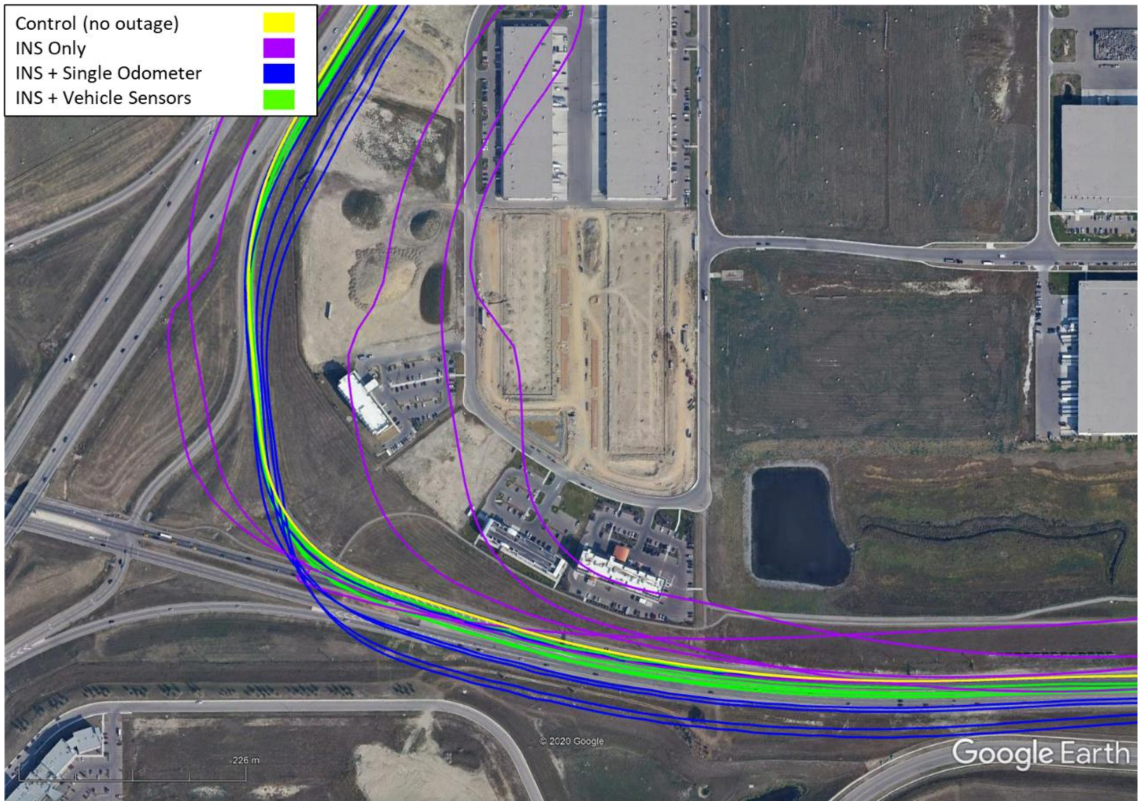

Figure 10 – Map View of 30-Minute GNSS Outage Performance, Mixed Driving Test, Zoomed [11]

Test 2: Extended GNSS Outages – Parking Lot Test

The second test scenario also takes place in an open sky environment but operates at much lower speeds to simulate driving within a parking structure. To ensure the most repeatable loop possible, the test vehicle was configured to use the drive-by-wire system to drive a pre-recorded loop autonomously. This scenario was made possible through access to a safe closed test site provided by the City of Calgary Living Labs program.

This test did not allow the car to stop at any point, which means that no zero velocity updates are available to the INS system, which makes this test case even more challenging for inertial navigation. This test is intended to show the effects of an extended GNSS outage on an auto-steer system exiting a parking structure. Autonomous systems have difficulty handling unstable position input as they will attempt to follow a very erratic path. The stability observed in the test above using vehicle sensors is therefore advantageous for this scenario.

As with the first test, the test unit is the same Hexagon | NovAtel PwrPak7-E1. Again, it is subjected to a 30-minute GNSS outage with the control unit providing the RTK reference trajectory. Unlike the first test though, the GNSS outage was imposed in real-time by unplugging the antenna of the test unit. The unaided INS and single odometer scenarios were post-processed from the recorded data, but the primary results were obtained in real-time. The auto-steering system did not have difficulty following the position trajectory thanks to its stability throughout the outage.

The 10-minute error statistics for this test are shown in Figure 11, Figure 12 and Table 4 below. The results echo the results seen in the previous test with increasing stability as more sensors are fused into the solution. In this test the 95% 2D position error remains within 1.5 metres, or within a lane for a full 10-minute outage.

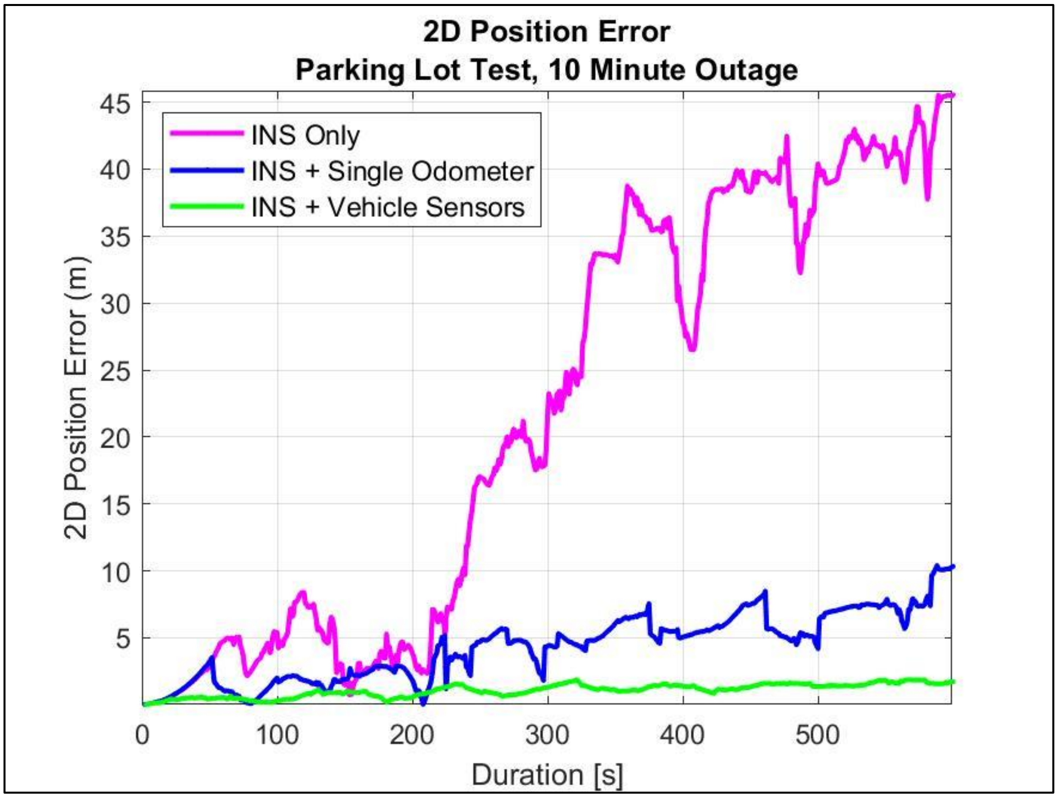

Figure 11 – 2D Position Error Over a 10 Minute GNSS Outage, Parking Lot Test

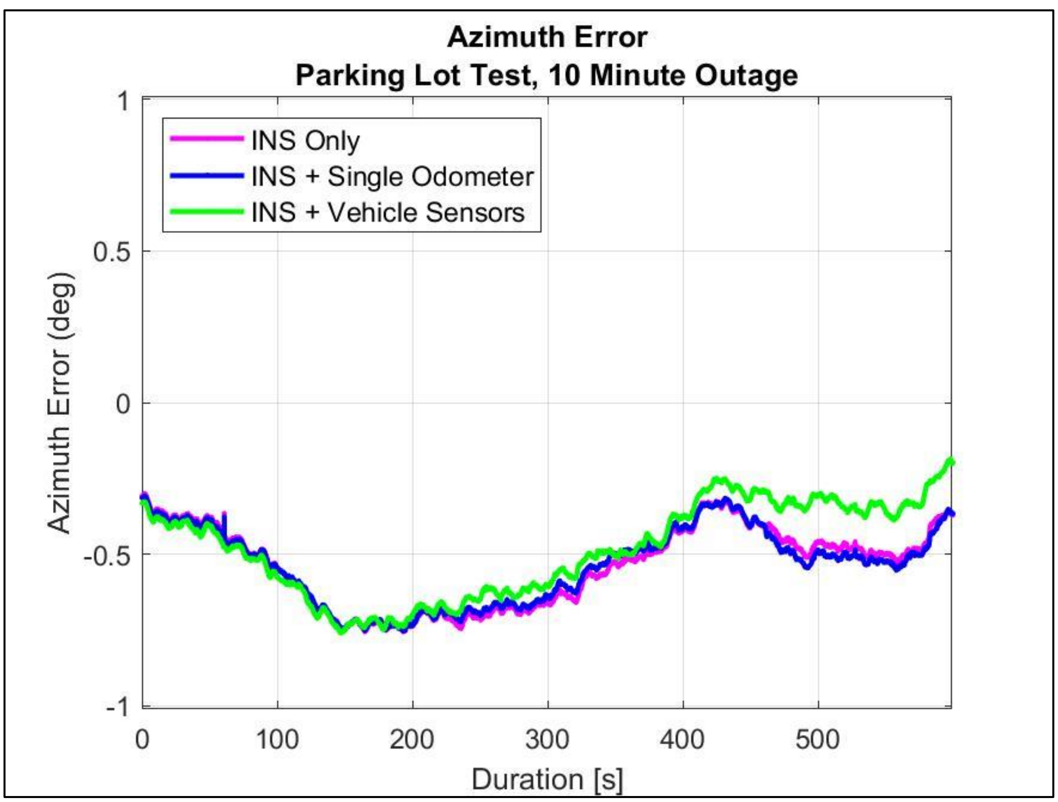

Figure 12 – Azimuth Error Over a 10 Minute GNSS Outage, Parking Lot Test

Table 4 10 Minute Outage Error Statistics, Parking Lot Test

Solution	RMS Error			95% Error		
	2D Position (m)	Height (m)	Azimuth (deg)	2D Position (m)	Height (m)	Azimuth (deg)
Unconstrained INS	648.08	32.06	0.13	1511.95	72.92	0.39
Land Profile – No DMI	27.04	2.92	0.13	48.35	5.14	0.39
Single Odometer	4.98	1.97	0.12	7.44	3.61	0.37
Vehicle Sensors	1.17	2.10	0.15	1.43	3.77	0.46

The full 30-minute error statistics are shown in Figure 13, Figure 14 and Table 5 below. The position accuracy remains strong throughout the full outage; however, a small but growing oscillation can be seen in the latter half of the outage. Correspondingly, the azimuth error begins to diverge specifically for the vehicle sensor data set. This is likely caused by errors in the relative yaw measurements from the vehicle sensors combined with the near constant turning of the parking test loops. These measurements begin to apply more weight to the INS solution as the outage continues and begin to bias the azimuth off. Despite this, the positioning error remains far better as multiple odometry provides better distance measurements will be better around those turns. Still, at the end of the 30-minutes, the 2D position error 95% is at only 5 metres, or 0.12% error / distance travelled (even though the total distance travelled is much lower in this test at about 6.5Km).

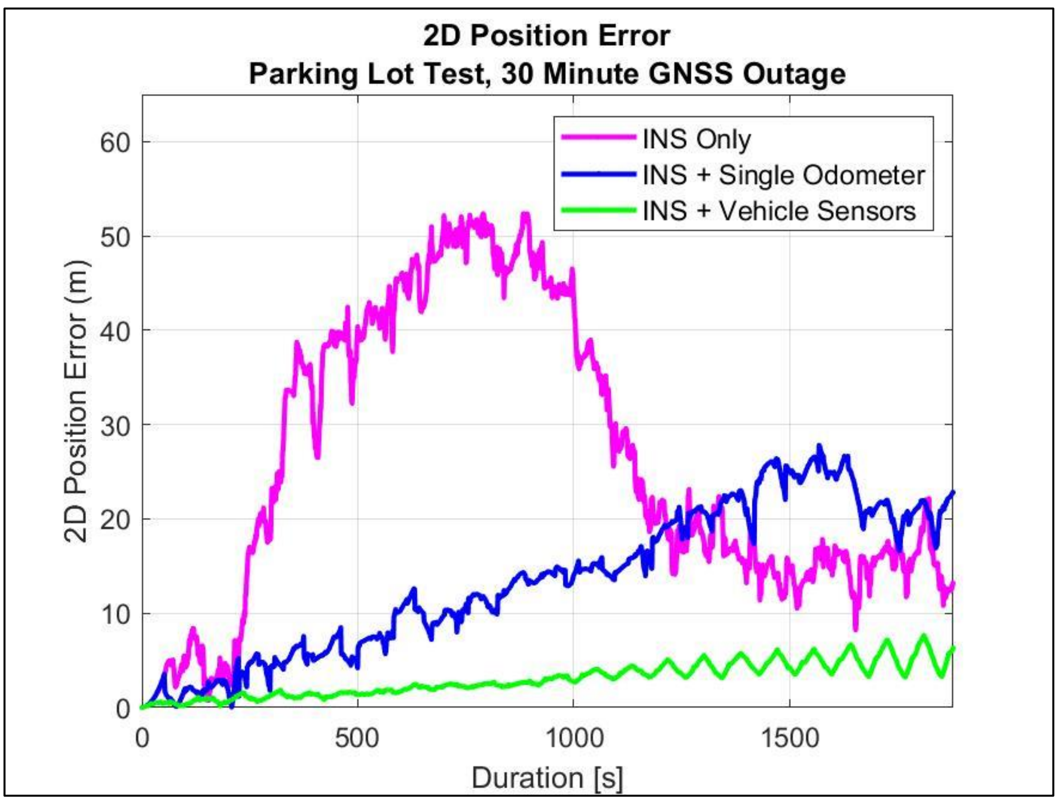

Figure 13 – 2D Position Error Over a 30 Minute GNSS Outage, Parking Lot Test

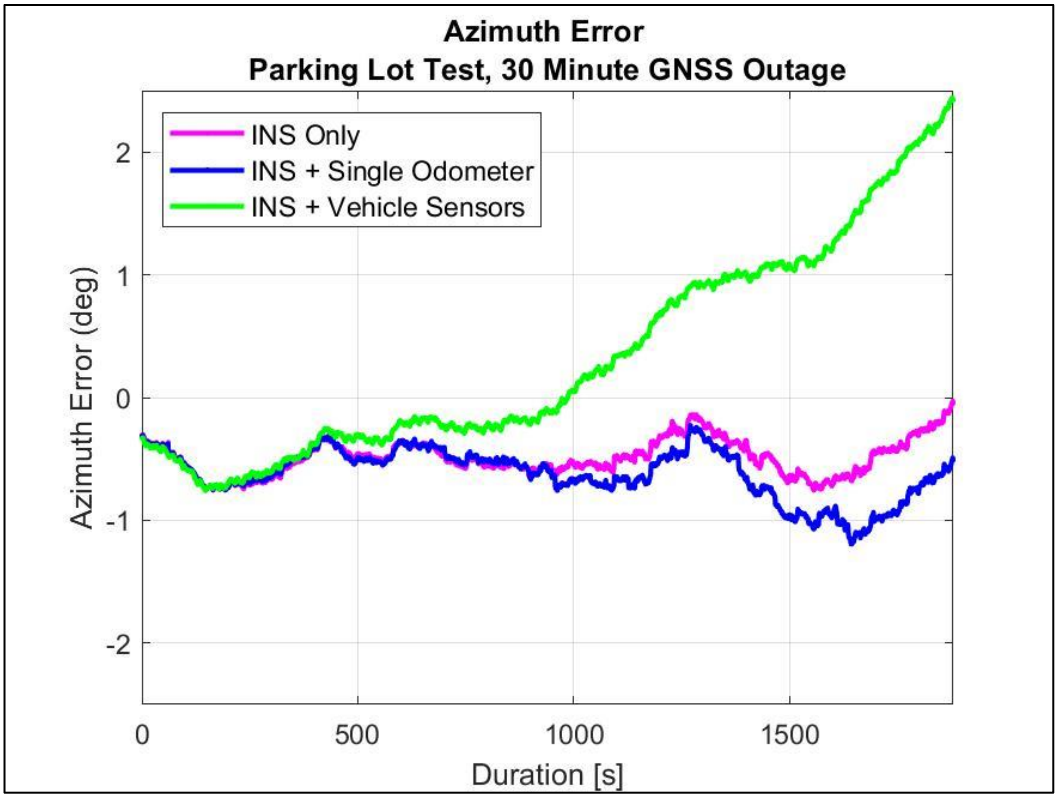

Figure 14 – Azimuth Error Over a 30 Minute GNSS Outage, Parking Lot Test

Table 5 30 Minute Outage Error Statistics, Parking Lot Test

Solution	RMS Error			95% Error		
	2D Position (m)	Height (m)	Azimuth (deg)	2D Position (m)	Height (m)	Azimuth (deg)
Land Profile – No DMI	30.19	11.10	0.14	46.05	18.46	0.43
Single Odometer	15.58	7.50	0.20	23.26	12.22	0.61
Vehicle Sensors	3.46	6.57	0.86	5.17	10.11	2.57

As with the first test, this can be looked at in a map view to get a context of the error growth over the full 30-minutes. This time because the vehicle was following the INS trajectory in real-time, the control line looks worse but represents where the vehicle actually drove while the real-time INS + vehicle sensor data shows what the INS solution was reporting, which was always following the original path. This test in the closed site is shown below in Figure 15.

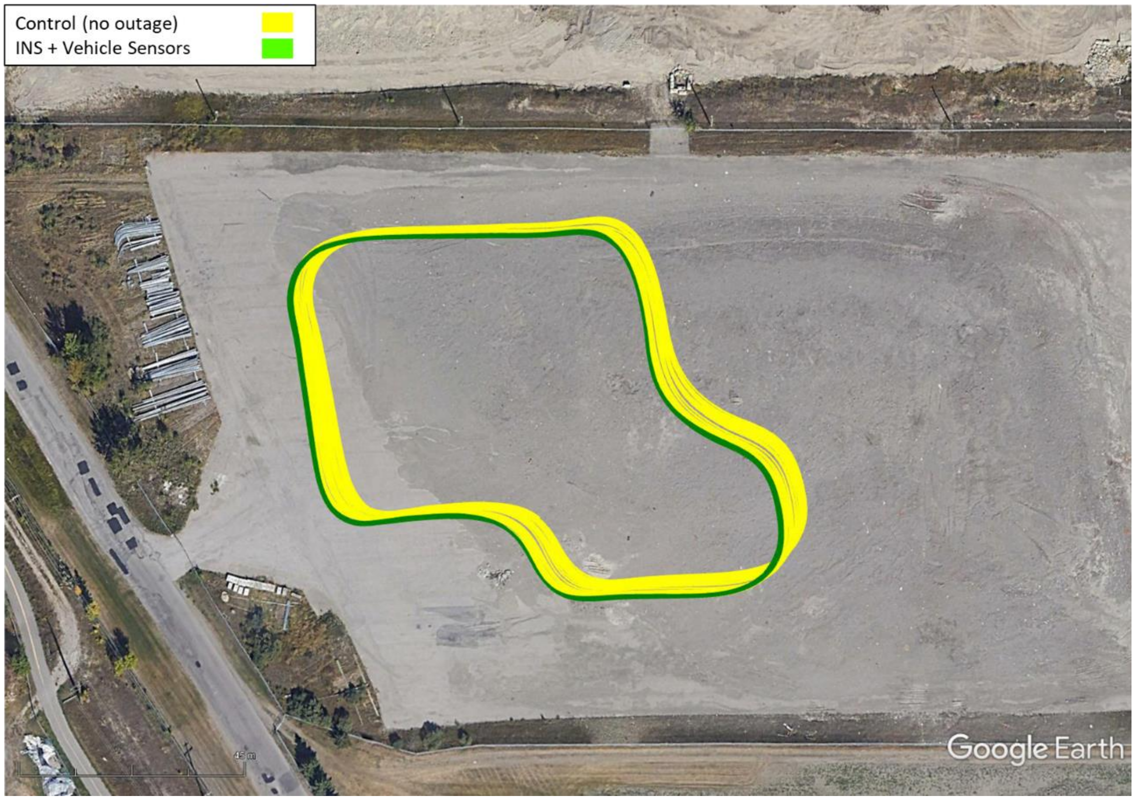

Figure 15 – Map View of 30-Minute GNSS Outage Performance, Parking Lot Test [11]

Test 3: Short Outages and Highway Test Using Automotive Grade Sensors

In the final test scenario, the NovAtel hardware is replaced by a low-cost, mass-market targeted sensor suite, representative of sensors that will be available for self-driving applications on autonomous passenger vehicles. RTK positioning is also replaced by Hexagon's fast-converging PPP service, TerraStar X, as PPP is the likely method for mass market deployment, due to its superior scalability among other factors.

GNSS and its supporting sensors provide the only source of absolute positioning for autonomous vehicles, making them a key component in a self-driving solution. Though vision sensors perform well in busy, urban environments, where GNSS struggles, they can struggle in open environments with fewer objects, or in adverse weather conditions, neither of which affect GNSS performance. For this reason, GNSS is particularly useful in highway environments. However, as shown previously [1,2], GNSS on its own cannot provide continuous PLs in the presence of highway overpasses or other partial or full obstructions. Again, IMUs are used to bridge these gaps. However, low-cost IMU errors grow too quickly for useable PLs in more challenging highway environments. This test will show that the addition of vehicle sensors can help to mitigate this problem.

Before studying the performance of the system on the highway, shorter GNSS outages will be examined by simulating several hundred 30 second outages. Figure 16 below shows the impact vehicle sensors have on the error profile. For very short GNSS outages, up to about 15 seconds, the IMU errors continue to dominate the performance. Starting at about 15 seconds, the vehicle sensors begin to significantly reduce error growth. The time of this transition will vary based on the quality of the IMU, the vehicle sensors and the conditions entering the outage. For the sensors used in this study, the highway environment errors are unlikely to be significantly affected, as the GNSS outages under bridges are typically on the order of 1-5 seconds.

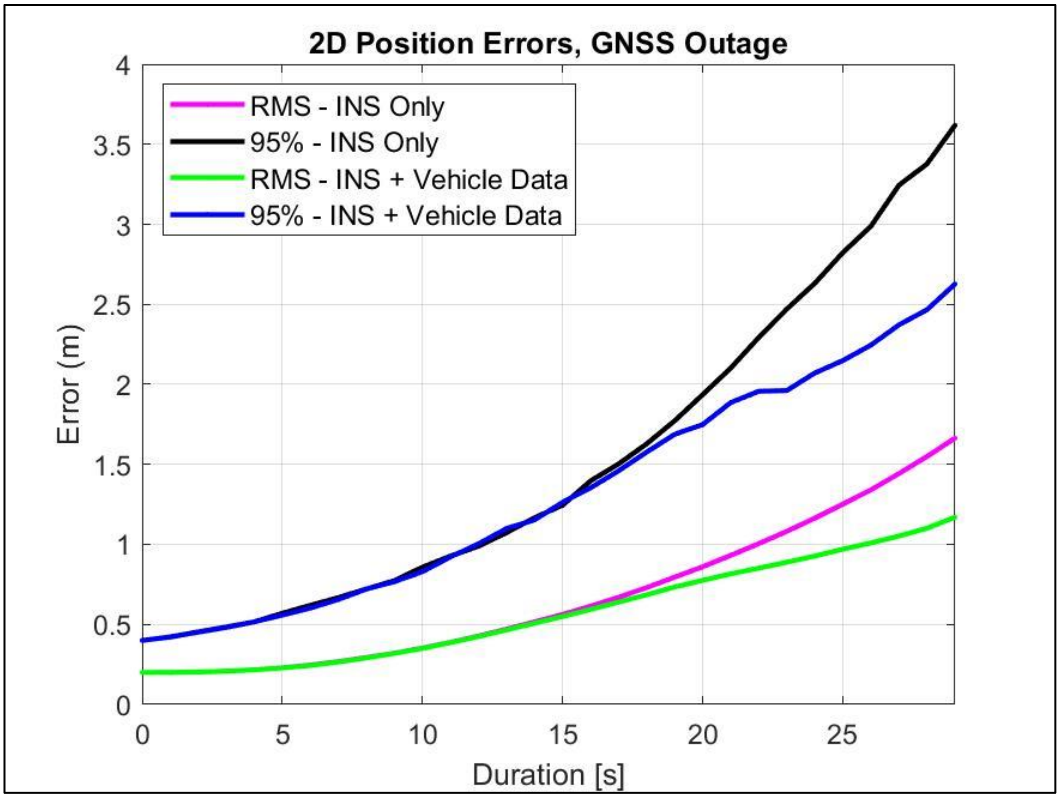

Figure 16 – Automotive Sensors Error over 30-Second GNSS Outages

Figure 17 shows the corresponding PL performance during the same GNSS outages. Unlike errors, the vehicle sensors have a significant and immediate effect on the PL. The contrast between the true error performance and the PL performance does make sense. In the case of the error profile, the performance is driven by the IMU at first, but as the IMU error states become less certain, the vehicle information begins to have a larger impact. This is because the vehicle sensor related error states tend to change more slowly. Conversely, in the case of PL growth, having a redundant source of information in the vehicle sensor data helps to constrain the maximum possible error that can be present in the system right away. Mathematically, the vehicle sensor inputs tend to agree well with the IMU observations at first, so the state is relatively unaffected, but since they provide a second source of observations, the covariance of the overall system is reduced, impacting the PL.

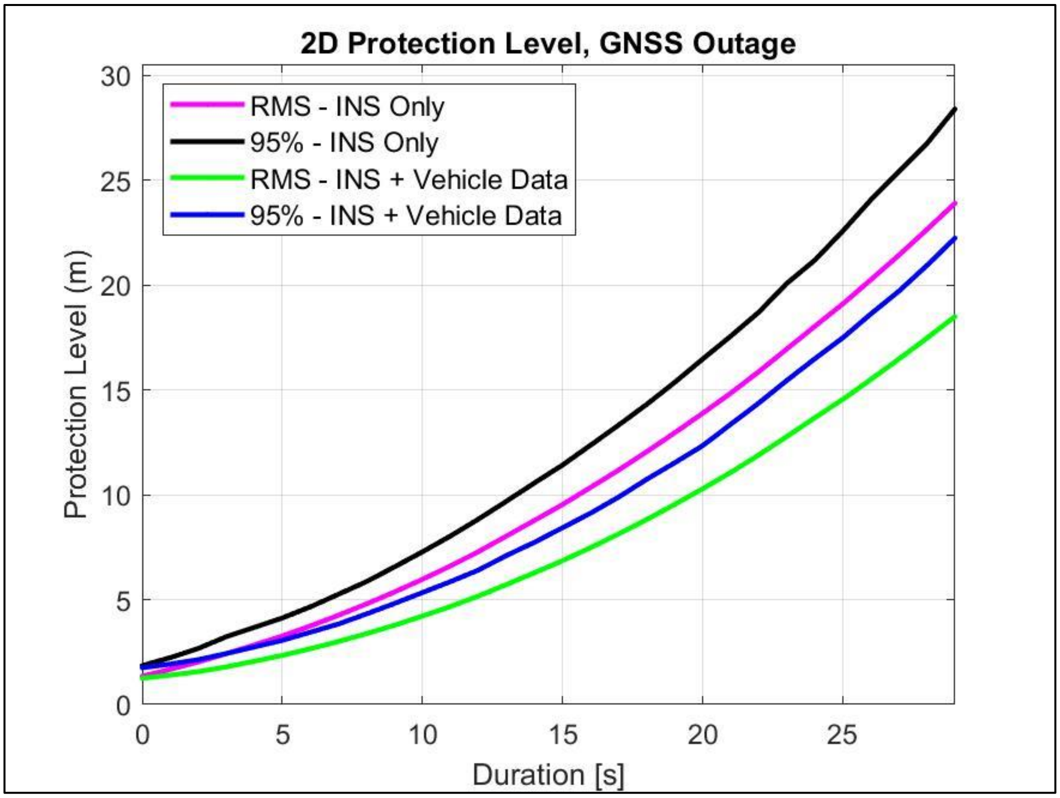

Figure 17 – Automotive Sensors Protection Level over 15-Second GNSS Outages

Table 6 below summarizes the data shown in Figure 16 and Figure 17. At 10 and 30-second GNSS outages the differences (or lack thereof) between errors and protection levels can be clearly seen.

Table 6 Automotive Sensors Error and Protection Level Statistics – 10 & 30 Second Outages

Solution	Outage Duration (s)	Error		Protection Level	
		2D Position RMS (m)	2D Position 95% (m)	2D Position RMS (m)	2D Position 95% (m)
IMU Only	10	0.15	0.46	4.62	5.43
Vehicle Sensors		0.15	0.43	2.96	3.56
IMU Only	30	1.57	3.42	23.89	28.68
Vehicle Sensors		1.05	2.59	18.32	21.81

Moving on from simulated outages to real conditions, highway data were collected on two major inter-city highways, which include overpasses at regular intervals, instances of multiple consecutive overpasses and some short underpass highway sections. Figure 18 shows the error and PL performance through the test; the left plot is the full dataset, and right is a zoomed in section to better show the behaviour as sky obstructions (overpasses) are encountered.

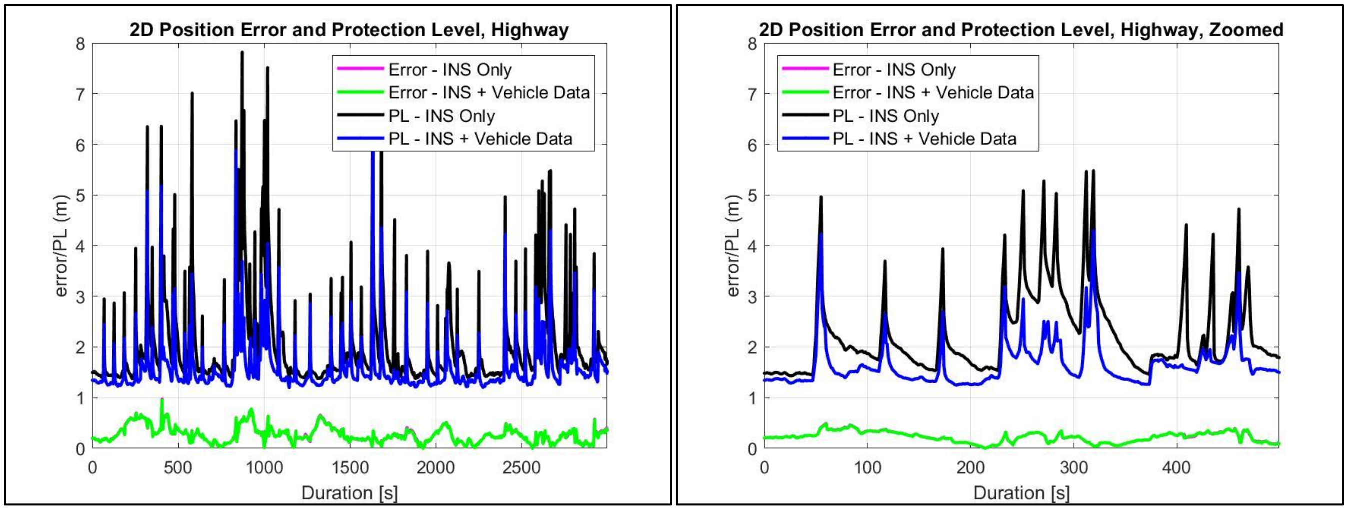

Figure 18 – Automotive Sensors Protection Level – Highway Driving

As expected from the short outage study above, the error profile is nearly identical, regardless of whether vehicle information is used or not. However, the contrast between the PL performance is significant. When using vehicle sensor data, protection levels remain lower overall, grow more slowly and recover faster. The redundant measurements provided allow for all three of these by providing additional information, which keeps the maximum possible error lower.

The faster recovery also compounds when encountering consecutive outages. In this case the PL recovers to a lower value between outages and therefore remains much more stable. This is highlighted in the zoomed-in portion of Figure 18. RMS and 95th percentile stats for the highway test are shown in Table 7.

Table 7 Automotive Sensors Error and Protection Level Statistics - Highway

Solution	Error		Protection Level	
	2D Position RMS (m)	2D Position 95% (m)	2D Position RMS (m)	2D Position 95% (m)
IMU Only	0.31	0.59	2.22	3.81
Vehicle Sensors	0.31	0.59	1.62	2.33

Since protection levels are only useful in autonomous applications when they are below the system defined alert limit, Table 8 summarizes the system availability, which is the percent of time that the system is below the corresponding alert limit. For challenging highway environments like the one studied here, vehicle information becomes more important for applications that require smaller alert limits.

Table 8 Automotive Sensors Availability at different Alert Levels - Highway

Solution	Availability (%)		
	2m Alert Level	3m Alert Level	5m Alert Level
IMU Only	69.2	88.6	98.3
Vehicle Sensors	90.8	98.1	99.8

A Stanford Plot [12] of the data assuming an alert limit of 3 m is shown below in Figure 19 both without (left) and with (right) vehicle sensor input. For both setup all points are in the upper left diagonal, supporting the algorithm validity. The different zones as labelled in the diagram are:

- Normal operation: The error is below the PL, and the PL is below the AL (available and safe)
- System unavailable: The error is below the PL, and the PL is above the AL (unavailable but safe)
- Misleading information (MI): The error is greater than the PL, and the error and PL are both below the AL (available and misleading, but not a safety risk because the error is less than the AL), or the error and PL are both above the AL (unavailable and misleading, but not a safety risk because the PL is greater than the AL)
- Hazardously misleading information (HMI): The error is greater than the AL and the PL is below the AL (unsafe)

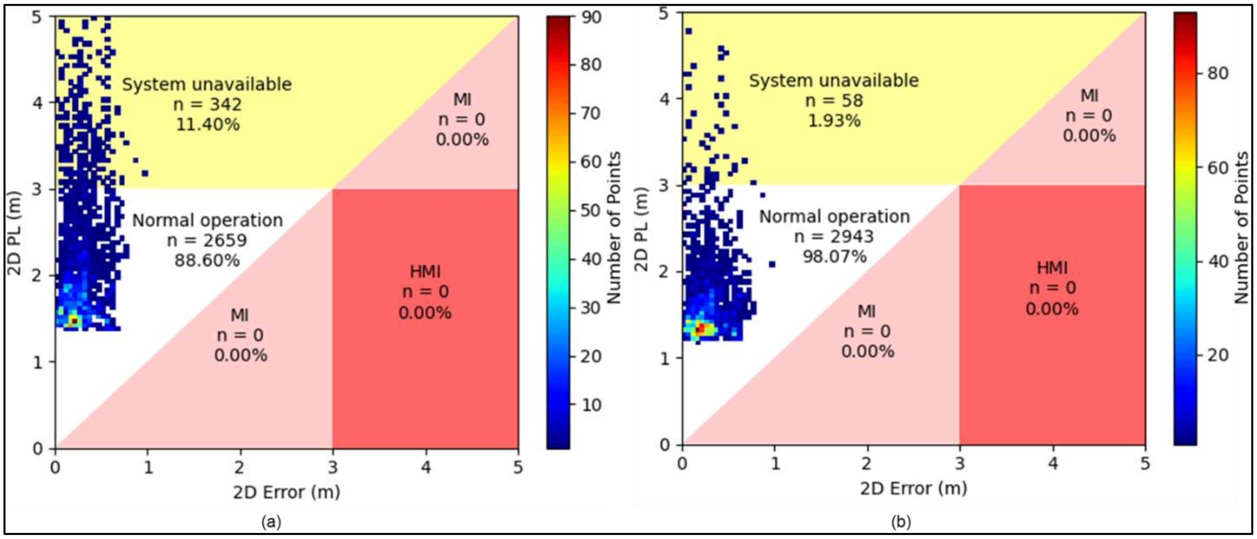

Figure 19 – Stanford Plot for 3m Safe Operation, (a) without and (b) with aiding vehicle sensor data

Importantly, no misleading positions are reported in either case, but the availability is significantly increased using the vehicle sensor data. This shows that adding vehicle sensor information has a significant impact on how often a functionally safe position can be made available in a typical autonomy application.

CONCLUSION

The results presented in this paper clearly show that there are compelling advantages to pairing existing vehicle sensors with an INS centric positioning system to boost positioning accuracy and availability. The accuracy benefits become more prevalent the longer that GNSS is unavailable, but protection levels are impacted over brief outages such as highway overpasses.

This is a very attractive proposition for autonomy applications as the sensors and data bus are already there in passenger vehicles. Modern vehicles in other industries, such as agriculture and mining, also possess many of these sensors and can benefit from this technique. Additionally, the computations necessary to add the sensors into an existing INS system are minimal and can also very likely be handled by processors already present on the existing system. This significantly improves system performance without any additional hardware cost.

Inertial navigation alone, even aided with vehicle sensor data, is not enough to maintain lane-level accuracy indefinitely, but it does significantly improve the accuracy, stability and safety throughout GNSS denied conditions, even for extended periods. This contributes to a more available safe solution for autonomy and a stronger core for further sensor fusion. Adding in additional data from visual sensors is also made easier with a more accurate and stable base. Either with map-matching or other visual sensor odometry, getting a solution agreement is more likely and more likely correct.

While a full autonomy stack will undoubtedly make use of a full sensor suite and high-definition maps, these test results show that existing sensors on vehicles can be harnessed to greatly improve performance without incurring any additional cost and with minimal knowledge of the vehicle platform.

REFERENCES

1. Norman, L., Infante, E., de Groot, L., “Integrity Performance for Precise Positioning in Automotive,” *International Meeting of the Satellite Division of the Institute of Navigation (ION GNSS+ 2019), Miami, FL, September 2019, pp. 1653 – 1663.*
2. Gunning, K., Blanch, J., Walter, T., de Groot, L., Norman, L., “Integrity for Tightly Coupled PPP and IMU,” *International Meeting of the Satellite Division of the Institute of Navigation (ION GNSS+ 2019), Miami, FL, September 2019, pp. 3066-3078.*
3. U.S. Department of Transportation. “Federal Motor Vehicle Safety Standards; Electronic Stability Control Systems; Controls and Displays,” Docket No. NHTSA-2007-27662, 2007.
4. European Parliament and the Council of The European Union. “Regulation (EC) No 661/2009 Concerning Type-Approval Requirements for the General Safety of Motor Vehicles, Their Trailers and Systems, Components and Separate Technical Units Intended Therefor,” 13 July 2009.
5. Groves, P., “Principles of GNSS, Inertial, and Multisensor Integrated Navigation Systems,” Second Edition. Boston, MA: Artech House, 2003.
6. Norris, W., “Modern Steam Road Wagons,” London, U.K.: Longman’s Green and Co., 1906, pp. 63-67
7. Dixon, R., Bobye, M., “Performance Differentiation in a Tightly Coupled GNSS/INS Solution,” *International Meeting of the Satellite Division of The Institute of Navigation (ION GNSS+ 2016), Portland, OR, pp. 2777 – 2788.*
8. ISO-11783 PGN9216 Tractor Implement Management Operation and Function Messages, External Guidance Curvature Request. https://www.isobus.net/isobus/pGNAndSPN/274
9. Dixon, R., Bobye, M., Kruger, B., Sinha, A., “GNSS/INS Fusion for Automotive with Mass Market Sensors,” *International Meeting of the Satellite Division of the Institute of Navigation (ION GNSS+ 2018), Miami, FL, September 2018, pp. 1497-1509.*
10. Sheridan, K., Alves, P., Masterson, S., Busser, J., Sadeque, Z., Gakne, P. L., “TerraStar X: Precise Point Positioning with Fast Convergence and Integrity”, *International Meeting of the Satellite Division of the Institute of Navigation (ION GNSS+ 2019), Miami, FL, September 2019, pp. 1916 – 1943.*
11. Image Source: Figure 9, Figure 10, Figure 15, *Google Earth* (satellite image August 31, 2017) Accessed August 26, 2020
12. Tossaint, M., Samson, J., Toran, F., Ventura-Traveset, J., Hernandez-Pajares, M., Juan, J.M., Sanz, J., Ramos-Bosch, P., "The Stanford - ESA Integrity Diagram: A New Tool for The User Domain SBAS Integrity Assessment", NAVIGATION, Journal of The Institute of Navigation, Vol. 54, No. 2, Summer 2007, pp. 153-162.